Available online at www.sciencedirect.com

SciVerse ScienceDirect

Ceramics International 38 (2012) 2593–2596

CERAMICS INTERNATIONAL

www.elsevier.com/locate/ceramint

Short communication

Major effects on varistor properties of $ZnO–V_2O_5–MnO_2–Nb_2O_5–Er_2O_3$ ceramics with sintering changes

Choon-W. Nahm *

Semiconductor Ceramics Laboratory, Department of Electrical Engineering, Dongeui University, Busan 614-714, Republic of Korea

Received 7 July 2011; received in revised form 12 October 2011; accepted 17 October 2011
Available online 23 October 2011

Abstract

The microstructure and electrical properties of $ZnO–V_2O_5–MnO_2–Nb_2O_5–Er_2O_3$ (ZVMNE) ceramics were investigated at different sintering temperatures (875–950 °C). The average grain size increased from 4.3 to 9.2 μm with the increase of sintering temperature. The breakdown field decreased from 7095 to 1256 V/cm with the increase of sintering temperature. The ZVMNE ceramics sintered at 900 °C exhibited a surprisingly high nonlinear coefficient (63). The donor concentration increased from 3.09×10^{17} to 7.99×10^{17} cm^{-3} with the increase of sintering temperature and the barrier height exhibited the maximum value (1.21 eV) at 900 °C.

Keywords: A. Sintering; B. Grain boundaries; C. Electrical properties; D. ZnO; E. Varistors

1. Introduction

Electronic systems are sensitive to both external and internal sources of overvoltage transients. This can be in the form of external electrostatic discharge or internally generated electrical fast transients. Transient voltages result from the sudden release of previously stored energy from lightning, inductive load switching, electromagnetic pulses or electrostatic discharges. Therefore, electrical and electronic systems should be protected from various surges. One way to overcome these surges is to enhance the insulating strength for devices and systems. Another way is to use the devices of protection against overvoltages that can use varistors. Varistors are variable resistors, which the resistance of a varistor varies automatically in response to change in voltages appearing across it.

Typical zinc oxide (ZnO) varistors are semiconducting ceramic devices made by sintering ZnO powders doped with main additives such Bi_2O_3 or Pr_6O_{11}, and subordinate additives such as CoO, MnO, Cr_2O_3, and Sb_2O_3. The boundaries between individual grains can be equated to pn junction with the entire mass represented as a series-parallel diode network. ZnO varistors can exhibit strong nonlinear properties, which give rise to abrupt decrease of impedance at critical voltage with the increase of voltage [1,2]. Owing to highly nonlinear properties, ZnO varistors has been extensively used in the field of circuit overvoltage protection, with application ranging from a few volts in electronic circuits to thousands of volts in electric power systems [3,4]. Commercial Bi_2O_3- and Pr_6O_{11}-based ZnO varistors cannot be co-fired with a silver inner-electrode (m.p. 961 °C) in a multilayered chip component because of their high sintering temperature above 1000 °C. New $ZnO–V_2O_5$-based ceramics can be sintered at a relatively low temperature of approximately 900 °C [5]. This is important for multilayer chip component applications, because it can be co-sintered with a silver inner-electrode without using expensive Pd or Pt, compared with commercial Bi_2O_3- and Pr_6O_{11}-based ceramics. A study of $ZnO–V_2O_5$-based ceramics is yet in its early stages in many points [6–12]. The $ZnO–V_2O_5$ -based ceramics requires specific additives and sintering process in order to exhibit higher nonlinear properties [13–16]. Therefore, it is very important to investigate the effects of sintering process on electrical properties for the varistor ceramics with specified composition. In this study, the effects of sintering on electrical properties of $ZnO–V_2O_5–MnO_2–Nb_2O_5–Er_2O_3$ (ZVMNE) ceramics was investigated and surprisingly high nonlinear coefficient (α) were obtained by proper sintering.

* Tel.: +82 51 890 1669; fax: +82 51 890 1664.
E-mail address: cwnahm@deu.ac.kr.

0272-8842/$36.00
doi:10.1016/j.ceramint.2011.10.050

2. Experimental procedure

Reagent-grade raw materials were prepared in the proportions of quaternary composition expression, such as 97.35 mol% ZnO + 0.5 mol% V_2O_5 + 2.0 mol% MnO_2 + 0.1 mol% Nb_2O_5 + 0.05 mol% Er_2O_3. Raw materials were mixed by ball milling with zirconia balls and acetone in a polypropylene bottle for 24 h. The mixture was dried at 120 °C for 12 h. The dried mixture mixed into container with acetone and 0.8 wt% polyvinyl butyral (PVB) binder of powder weight. After drying, the mixture was granulated by sieving 100-mesh screen to produce starting powder. The powder was uniaxially pressed into discs of 10 mm in diameter and 1.5 mm in thickness at a pressure of 100 MPa. The discs were covered with raw powder in alumina crucible, sintered at four fixed sintering temperatures (875 °C, 900 °C, 925 °C, and 950 °C) in air for 3 h, and furnace-cooled to room temperature. The final samples were about 8 mm in diameter and 1.0 mm in thickness. Silver paste was coated on both faces of the samples and the electrodes were formed by heating it at 550 °C for 10 min. The electrodes were 5 mm in diameter.

The surface microstructure was examined by a field emission scanning electron microscope (FESEM, Quanta 200, FEI, Brno, Czech). The average grain size (d) was determined by the linear intercept method [17]. The crystalline phases were identified by X-ray diffractometer (XRD, X′pert-PRO MPD, Panalytical, Almelo, Netherland) with CuK_α radiation. The sintered density (ρ) was measured using a density determination kit (238490) attached to balance (AG 245, Mettler Toledo International Inc., Greifensee, Switzerland).

The electric field–current density (E–J) characteristics were measured using a V–I source (Keithley 237, Keithley Instruments Inc., Cleveland, OH, USA). The breakdown field ($E_{1\ \mathrm{mA}}$) was measured at a current density of 1.0 mA/cm^2 and the leakage current density (J_L) was measured at 0.80 $E_{1\ \mathrm{mA}}$. In addition, the non-ohmic coefficient (α) was determined from $\alpha = 1/(\log E_2 - \log E_1)$, where E_1 and E_2 are the electric fields corresponding to 1.0 mA/cm^2 and 10 mA/cm^2, respectively.

The capacitance–voltage (C–V) characteristics of were measured at 1 kHz using an RLC meter (QuadTech 7600, Marlborough, MA, USA) and an electrometer (Keithley 617, Keithley Instruments Inc., Cleveland, OH, USA). The donor density (N_d) and the barrier height (Φ_b) were determined by the equation $(1/C_b - 1/2C_{bo})^2 = 2(\Phi_b + V_{gb})/q\varepsilon N_d$ [18], where C_b is the capacitance per unit area of a grain boundary, C_{bo} is the value of C_b when $V_{gb} = 0$, V_{gb} is the applied voltage per grain boundary, q is the electronic charge, ε is the permittivity of ZnO ($\varepsilon = 8.5\varepsilon_o$). The density of interface states (N_t) at the grain boundary was determined by the equation: $N_t = (2\varepsilon N_d \Phi_b/q)^{1/2}$ [18].

3. Results and discussion

Fig. 1 shows the SEM micrographs of the ZVMNE ceramics with different sintering temperatures. The grain structure is very homogeneously distributed and the grain boundaries are clear throughout all the ceramics, compared with existing reported literature [5–12]. The average grain size of the ZVMNE ceramics increased from 4.3 to 9.2 μm with the increase of sintering temperature. ZnO grains could probably grow rapidly in the presence of a rich liquid phases related to V_2O_5 because the melting point of V_2O_5 is 690 °C. The sintered density of the ZVMNE ceramics decreased from 5.56 to 5.46 g/cm^3 corresponding to 96.2–94.5% of the theoretical

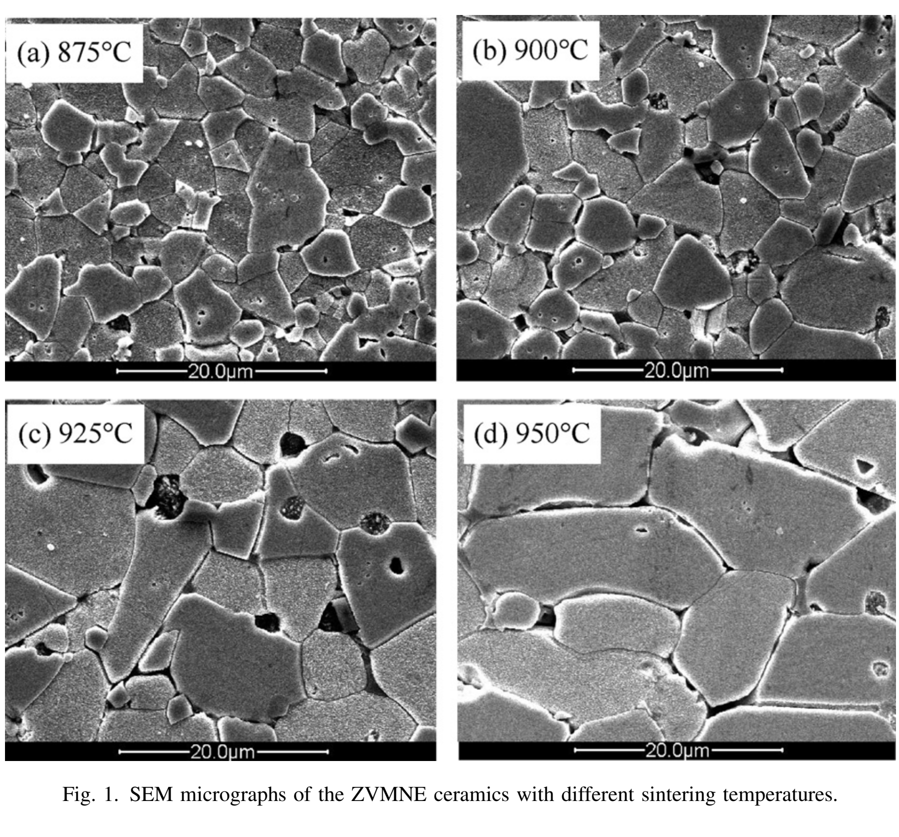

Fig. 1. SEM micrographs of the ZVMNE ceramics with different sintering temperatures.

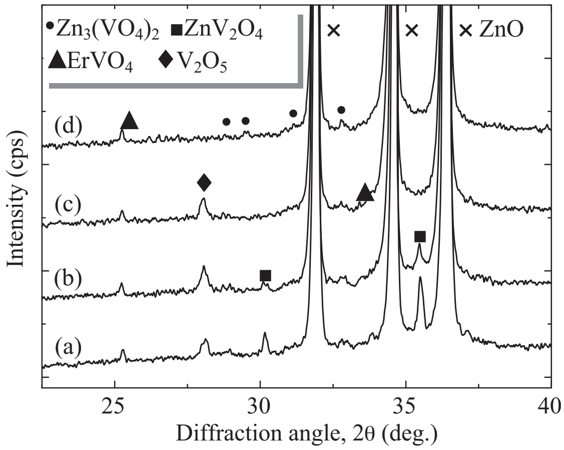

Fig. 2. XRD patterns of the ZVMNE ceramics with different sintering temperatures: (a) 875 °C, (b) 900 °C, (c) 925 °C, and (d) 950 °C.

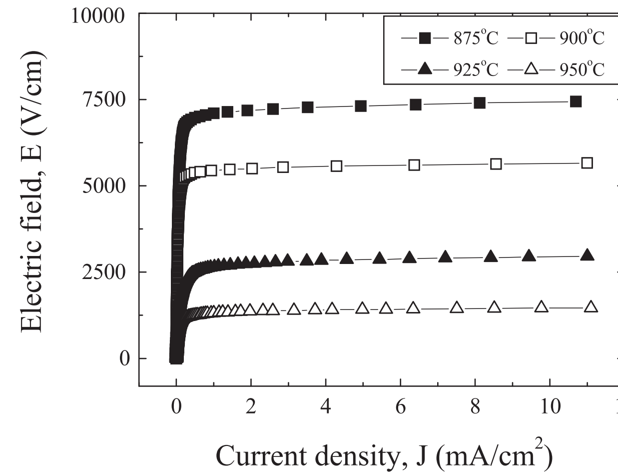

Fig. 3. *E–J* characteristics of the ZVMNE ceramics with different sintering temperatures.

density (TD) (pure ZnO, TD = 5.78 g/cm^3) with the increase of sintering temperature. It is assumed that the decrease of sintered density is attributed to the volatility of the V-species for V_2O_5 with low melting point.

The XRD patterns of the ZVMNE ceramics with different sintering temperatures are shown in Fig. 2. These patterns revealed the presence of $Zn_3(VO_4)_2$, ZnV_2O_4, and $ErVO_4$ as minor secondary phases, which act as liquid-phase sintering aids, in addition to a major phase of hexagonal ZnO [14]. The detailed microstructure parameters are summarized in Table 1.

Fig. 3 shows the electric field–current density (*E–J*) characteristics of the ZVMNE ceramics with different sintering temperatures. The varistor properties are featured by the conduction characteristics, which do not follow ohm's law in the *E–J* relation. The curves are divided into two regions: one is a linear region with very high resistance before breakdown field and another is a nonlinear region with very low resistance after breakdown field. The sharp knee of the curves leads to the better varistor properties. The *E–J* characteristic parameters are summarized in Table 1.

The breakdown field ($E_{1\ mA}$) linearly decreased from 7095 to 1256 V/cm with the increase of sintering temperature. The behavior of $E_{1\ mA}$ in accordance with sintering temperatures can be explained by the following expression: $E_{1\ mA} = v_b/d$, where d is the grain size and v_b is the breakdown voltage per grain boundaries. This expression indicated that the d and v_b values directly determine $E_{1\ mA}$. Therefore, the decrease of $E_{1\ mA}$ with the increase of sintering temperature is attributed to the increase of the average ZnO grain size from 4.3 to 9.3 μm and the decrease of breakdown voltage per grain boundaries from 3.0 to 1.1 V/gb. The nonlinear coefficient (α) increased from 50 to 63 with the increase of sintering temperature up to 900 °C. However, further increase in sintering temperature caused α to decrease to 15 at 950 °C. It should be noted that the ZVMNE ceramics sintered at 900 °C exhibited a maximum value ($\alpha = 63$) in the $ZnO–V_2O_5$-based varistors reported until now [5–16]. Therefore, this may be tuning point in the $ZnO–V_2O_5$-based varistor development of high performance as a new composition. As a result, it can be seen that the sintering temperature has a significant effect on the nonlinear properties of these ceramics in the light of the α variation. The behavior of α in accordance with sintering temperature can be related to the variation of the Schottky barrier height according to the variation of the electronic states at the grain boundaries. The sintering temperature will vary the density of interface states with the transport of the defect ions toward the grain boundary and will be more active grain boundaries. Therefore, the decrease of α with the increase of sintering temperature beyond 900 °C is attributed to the decrease of potential barrier height at the grain boundaries. On the whole, the leakage current density (J_L) exhibited much higher values compared with other kinds of varistor ceramics and this is a problem to work out in the near future.

Fig. 4 shows the capacitance–voltage (*C–V*) characteristics of the ZVMNE ceramics with different sintering temperatures. The detailed *C–V* characteristic parameters, such as donor concentration (N_d), barrier height (Φ_b), and density of interface states (N_t) are summarized in Table 1. The N_d increased from

Table 1
Microstructure, *V–I*, and *C–V* characteristic parameters of the ZVMNE ceramics for different sintering temperatures.

Sintering temp. (°C)	d (μm)	ρ (g/cm^3)	$E_{1\ mA}$ (V/cm)	v_b (V/gb)	α	J_L (μA/cm^2)	N_d (10^{17} cm^{-3})	Φ_b (eV)	N_t (10^{12} cm^{-2})
875	4.3	5.56	7095	3.0	50	94.1	3.09	1.06	1.75
900	5.2	5.53	5444	2.8	63	73.0	4.41	1.21	2.24
925	7.1	5.50	2649	1.9	22	218.2	5.47	0.79	2.02
950	9.2	5.46	1256	1.1	15	105.5	7.99	0.52	1.97

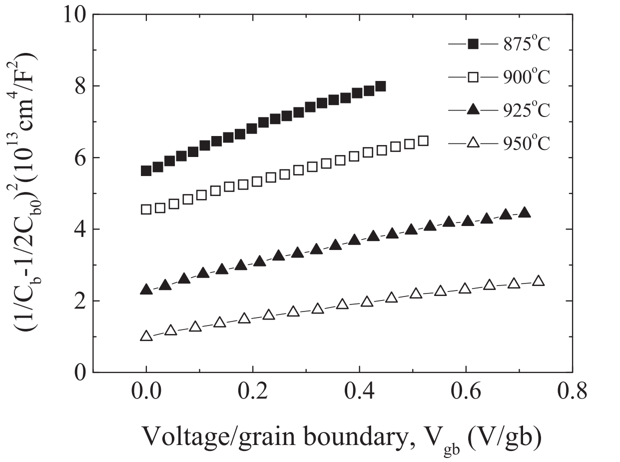

Fig. 4. *C–V* characteristics of the ZVMNE ceramics with different sintering temperatures.

3.09×10^{17} to 7.99×10^{17} cm^{-3} with the increase of sintering temperatures. The increase of N_d value is assumed to be due to the dissociation of zinc oxide in the following chemical reaction expression, $ZnO \rightarrow Zn_i^x + 1/2O_2$, $Zn_i^x \rightarrow Zn_i^{\bullet} + e'$, where Zn_i^x is a neutral zinc of interstitial site, $Zn_i^{\bullet}$ is a positively charged zinc ion of interstitial site. It is assumed that the enhancement of the donor density results from a lot of dissociation quantities of zinc oxide when the sintering temperature increases [19]. The barrier height (Φ_b) at the grain boundaries increased from 1.06 to 1.21 eV with the increase of sintering temperature up to 900 °C. However, further increase in sintering temperature caused Φ_b to decrease to 0.52 eV at 950 °C. The behavior of Φ_b in accordance with sintering temperatures exhibited to accord to the behavior of N_t at the grain boundaries. The behavior of Φ_b and N_t coincides with the behavior of α in the *E–J* characteristics. Really, the higher barrier gives rise to the higher nonlinear coefficient.

4. Conclusions

The microstructure and electrical properties of $ZnO–V_2O_5–MnO_2–Nb_2O_5–Er_2O_3$ (ZVMNE) ceramics were investigated at different sintering temperatures (875–950 °C). The average grain size increased from 4.3 to 9.2 μm with the increase of sintering temperature. The breakdown field decreased from 7095 to 1256 V/cm with the increase of sintering temperature. The ZVMNE ceramics sintered at 900 °C exhibited surprisingly high nonlinear coefficient of 63. The donor concentration increased from 3.09×10^{17} to 7.99×10^{17} cm^{-3} with the increase of sintering temperature and the barrier height exhibited the maximum value (1.21 eV) at 900 °C. Conclusively, it is believed that ZVMNE ceramics will be applied to the development of advanced varistors.

References

[1] M. Matsuoka, Nonohmic properties of zinc oxide ceramics, Jpn. J. Appl. Phys. 10 (1971) 736–746.
[2] H.R. Pilipp, L.M. Levinson, The physics of metal oxide varistors, J. Appl. Phys. 46 (1976) 1332–1341.
[3] L.M. Levinson, H.R. Philipp, Zinc oxide varistor – a review, Am. Ceram. Soc. Bull. 65 (1986) 639–646.
[4] T.K. Gupta, Application of zinc oxide varistor, J. Am. Ceram. Soc. 73 (1990) 1817–1840.
[5] J.-K. Tsai, T.-B. Wu, Non-ohmic characteristics of $ZnO–V_2O_5$ ceramics, J. Appl. Phys. 76 (1994) 4817–4822.
[6] J.-K. Tsai, T.-B. Wu, Microstructure and nonohmic properties of binary $ZnO–V_2O_5$ ceramics sintered at 900 °C, Mater. Lett. 26 (1996) 199–203.
[7] C.T. Kuo, C.S. Chen, I.-N. Lin, Microstructure and nonlinear properties of microwave-sintered $ZnO–V_2O_5$ varistors: I. Effect of V_2O_5 doping, J. Am. Ceram. Soc. 81 (1998) 2942–2948.
[8] H.-H. Hng, K.M. Knowles, Microstructure and current–voltage characteristics of multcomponent vanadium-doped zinc oxide varistors, J. Am. Ceram. Soc. 83 (2000) 2455–2462.
[9] H.-H. Hng, P.L. Chan, Effects of MnO_2 doping in V_2O_5-doped ZnO varistor system, Mater. Chem. Phys. 75 (2002) 61–66.
[10] H.-H. Hng, P.L. Chan, Microstructure and current–voltage characteristics of $ZnO–V_2O_5–MnO_2$ varistor system, Ceram. Int. 30 (2004) 1647–1653.
[11] C.-W. Nahm, Microstructure and varistor properties of $ZnO–V_2O_5–MnO_2$-based ceramics, J. Mater. Sci. 42 (2007) 8370–8373.
[12] H.-H. Hng, P.L. Chan, Cr_2O_3 doping in ZnO–0.5 mol% V_2O_5 varistor ceramics, Ceram. Int. 35 (2009) 409–413.
[13] C.-W. Nahm, Preparation and varistor properties of new quaternary Zn–V–Mn–(La, Dy) ceramics, Ceram. Int. 35 (2010) 3435–3440.
[14] C.-W. Nahm, Effect of dopant (Al, Nb, Bi, La) on varistor properties of $ZnO–V_2O_5–MnO_2–Co_3O_4–Dy_2O_3$ ceramics, Ceram. Int 36 (2010) 1109–1115.
[15] C.-W. Nahm, Influence of Nb addition on microstructure, electrical, dielectric properties, and aging behavior of MnCoDy modified Zn–V-based varistors, J. Mater. Sci.: Mater. Electron. 21 (2010) 540–547.
[16] C.-W. Nahm, DC accelerated aging behavior of Co–Dy–Nb doped Zn–V–M-based varistors with sintering process, J. Mater. Sci.: Mater. Electron. 22 (2011) 444–451.
[17] J.C. Wurst, J.A. Nelson, Lineal intercept technique for measuring grain size in two-phase polycrystalline ceramics, J. Am. Ceram. Soc. 55 (1972) 109–111.
[18] M. Mukae, K. Tsuda, I. Nagasawa, Capacitance-vs-voltage characteristics of ZnO varistors, J. Appl. Phys. 50 (1979) 4475–4476.
[19] M.F. Yan, A.H. Heuer, Additives and Interfaces in Electronic Ceramics, Am. Ceram. Soc., Columbus, OH, 1983, p. 80.